Precambrian Research 289 (2017) 62–74

Contents lists available at ScienceDirect

Precambrian Research

journal homepage: www.elsevier.com/locate/precamres

Rock magnetic cyclostratigraphy of the Doushantuo Formation, South China and its implications for the duration of the Shuram carbon isotope excursion

Zheng Gong [a,*], Kenneth P. Kodama [a], Yong-Xiang Li [b]

[a] Department of Earth and Environmental Sciences, Lehigh University, 1 West Packer Avenue, Bethlehem, PA 18015, USA
[b] State Key Laboratory for Mineral Deposits Research, School of Earth Sciences and Engineering, Nanjing University, 163 Xianlin Avenue, Nanjing 210023, China

ARTICLE INFO

Article history:
Received 22 June 2016
Revised 11 November 2016
Accepted 8 December 2016
Available online 20 December 2016

Keywords:
Shuram excursion
Carbon isotope
Ediacaran
Doushantuo Formation
South China
Rock magnetic cyclostratigraphy

ABSTRACT

The Shuram excursion (SE), one of the largest-known negative carbon isotope anomalies, has been globally observed in Ediacaran rocks. Precisely determining the duration of the SE is pivotal to understanding its controversial origin. Here, we present a detailed paleomagnetic, rock magnetic, cyclostratigraphic and carbon isotopic study of the SE in the Doushantuo Formation at the Dongdahe section in eastern Yunnan Province, South China. Although paleomagnetic results likely show a late Mesozoic remagnetization, careful mineralogic analyses indicate that the rock magnetic cyclostratigraphy carried by detrital pseudo-single domain (SD) or small multidomain (MD) titanomagnetite grains faithfully records orbitally-forced climate cycles in the Ediacaran. Multi-taper method (MTM) spectral analysis of magnetic susceptibility (MS) and anhysteretic remanent magnetization (ARM) series reveals significant spectral peaks at similar frequencies. Based on the ratios of their frequencies, these spectral peaks are assigned to a suite of Milankovitch cycles (long eccentricity, short eccentricity, obliquity and precession), yielding a sediment accumulation rate of 1.0 cm/kyr for the Doushantuo Formation. A 9.1 ± 1.0 Myr duration is indicated for the entire SE in South China. This result is in good agreement with independent estimates from North America and South Australia, thus supporting a primary origin for the SE. In combination with published geochronologic data, we suggest that the onset of the SE occurred at ca. 560 Ma, which provides a chronostratigraphic framework for evaluating the relationship between the SE and the evolution of metazoans in Ediacaran time.

1. Introduction

The Ediacaran Period (ca. 635–541 Ma; Knoll et al., 2006) witnessed one of the largest negative carbon isotope anomalies in Earth history, the Shuram excursion (SE). The SE is distinguished by its pronounced depletion in $\delta^{13}C$ values (as low as −12‰), expanded stratigraphic record and global distribution (Grotzinger et al., 2011). The origin of the SE remains enigmatic because the depleted $\delta^{13}C$ values should have exhausted the available oxidant budget based on the modeling of the Ediacaran carbon cycle (Bristow and Kennedy, 2008). A range of qualitative and quantitative models have been proposed to explain the anomalous $\delta^{13}C$ values (Rothman et al., 2003; Knauth and Kennedy, 2009; Derry, 2010; Bjerrum and Canfield, 2011). Nonetheless, there is no consensus regarding whether the SE represents a primary perturbation of the Ediacaran carbon cycle, or a secondary alteration during diagenesis (Grotzinger et al., 2011).

It is hypothesized that there is a causal link between the SE and the evolution of metazoans in Ediacaran time (Condon et al., 2005; Zhu et al., 2007). This assertion is based on the assumption that the SE was produced by the oxidation of organic carbon in the deep ocean, coeval with the rise of the atmospheric oxygen content during late Neoproterozoic time (Fike et al., 2006; Canfield et al., 2007; McFadden et al., 2008). A detailed chronostratigraphic framework is important to understand the controversial origin of the SE, with its implications for the evolution of metazoans. If the SE represents a primary depositional event, it should be globally correlative in both chronostratigraphy and duration. Due to the lack of robust biostratigraphic and radiometric age constraints, global chronostratigraphic correlations of the SE are based almost exclusively on chemostratigraphy (Grotzinger et al., 2011). The duration of the SE has been directly estimated in North America (Minguez et al., 2015), Oman (Le Guerroué et al., 2006; Bowring et al.,

* Corresponding author.
E-mail address: njugongzheng@gmail.com (Z. Gong).

http://dx.doi.org/10.1016/j.precamres.2016.12.002
0301-9268/

2007), South Australia (Minguez and Kodama, submitted for publication), and Siberia (Melezhik et al., 2009). An ~8 Myr duration of the SE has been consistently observed by rock magnetic cyclostratigraphic studies from the Johnnie Formation of the Death Valley region, North America and the Wonoka Formation, South Australia (Minguez et al., 2015; Minguez and Kodama, submitted for publication). Besides, a reversed-to-normal geomagnetic polarity transition was discovered at the nadir of the SE in both the Johnnie and Wonoka formations, supporting the global synchroneity of the SE (Minguez et al., 2015; Minguez and Kodama, submitted for publication).

Only a few chronostratigraphic studies have been conducted in South China, where the SE has been widely observed in the fossiliferous Doushantuo Formation across the Yangtze carbonate platform (Condon et al., 2005; Zhu et al., 2007; Lu et al., 2013). On the basis of zircon U-Pb age constraints from the Yangtze Gorges area, Condon et al. (2005) estimated that the SE lasted for 1–10 Myr and terminated at ca. 551 Ma. A recent Sr isotopic study suggests that the duration of the SE ranges from 15 to 30 Myr (Cui et al., 2015). Such estimates have considerable uncertainties and are not sufficiently precise for global correlations, pointing to the need for a high-resolution study of the duration of the SE in South China. In addition, only one geomagnetic reversal has been reported by previous paleomagnetic studies of the Doushantuo Formation, which, however, is stratigraphically close to the termination of the SE (Zhang et al., 2015). Hence, it is important to study a different section of the SE in South China to test if the reversed-to-normal geomagnetic reversal can be observed at the nadir of the SE as the cases in North America and South Australia.

In this paper, we present a detailed paleomagnetic, rock magnetic, cyclostratigraphic and carbon isotopic study of the Doushantuo Formation at the Dongdahe section in eastern Yunnan Province, South China. Paleomagnetic results indicate a late Mesozoic remagnetization, but rock magnetic cyclostratigraphy is carried by detrital PSD or small MD titanomagnetite grains, which faithfully records orbitally-forced climate cycles in the Ediacaran. The duration of the SE that we estimate from South China is in good agreement with those from North America and South Australia, consistent with a primary origin for this carbon isotope anomaly. Combining the estimated duration of the SE with published geochronologic data, we propose that the onset of the SE occurred at ca. 560 Ma, thus providing an Ediacaran chronostratigraphic framework for evaluating the relationship between the SE and the evolution of metazoans.

2. Geologic background

The Ediacaran sequence on the Yangtze carbonate platform in South China consists of the Doushantuo and Dengying formations, both of which were deposited on a rifted continental margin after the breakup of the Neoproterozoic supercontinent Rodinia (Wang and Li, 2003). Occurring stratigraphically between the Cryogenian Nantuo diamictite and the Ediacaran Dengying dolostone, the Ediacaran Doushantuo Formation is usually divided into four stratigraphic members based on facies variations (Jiang et al., 2011). Two lithologic marker beds, the cap carbonate (Member I) at the base and the organic-rich black shale (Member IV) at the top of the Doushantuo Formation, are widely used in stratigraphic correlations across the Yangtze carbonate platform in South China (Jiang et al., 2011). The Doushantuo Formation hosts three negative carbon isotope excursions, among which the one with the most depleted $\delta^{13}C$ values in Doushantuo Members III and IV is regarded as equivalent to the SE (Zhu et al., 2007; McFadden et al., 2008). The age of the Doushantuo-Dengying boundary is constrained to be 551.1 ± 0.7 Ma based on zircon U-Pb dates from an ash layer in the Yangtze Gorges area (Condon et al., 2005) and has been widely regarded as the termination age of the SE (Zhu et al., 2007; Fike et al., 2006; Grotzinger et al., 2011; Lu et al., 2013).

Previous studies show that the Dongdahe section (24°42.169′N, 102°57.115′E; Fig. 1) was paleogeographically located at the southwestern margin of the Yangtze carbonate platform in a shallow-water basin environment (Jiang et al., 2011; Lu et al., 2013). Here, the Doushantuo Formation is about 180 m in thickness and consists of 50-m of brownish sandstone and silty shale (Member I); approximately 120-m of thickly-bedded dolostone, interbedded shale and thinly-bedded, laminated muddy limestone (Members II and III); and an 8-m black shale (Member IV; Zhu et al., 2007). The entire SE is recorded in 91.2 ± 9.5 m of the Doushantuo Members III and IV at the Dongdahe section (Zhu et al., 2007). Uncertainty in the stratigraphic thickness results from the poor exposure of the onset of the SE in the Dongdahe section (Fig. 2B). In the field, the lower Dongdahe section is inaccessible because it is exposed in a cliff, prohibiting stratigraphically continuous sampling of this part of the SE. The upper Dongdahe section, which includes the upper Doushantuo Member III and the entire Doushantuo Member IV, is along a roadcut with a mean bedding dipping to the east (Strike = 9°NE, Dip = 40°E) and has a stratigraphic thickness of 53 m. Regional geologic investigations show

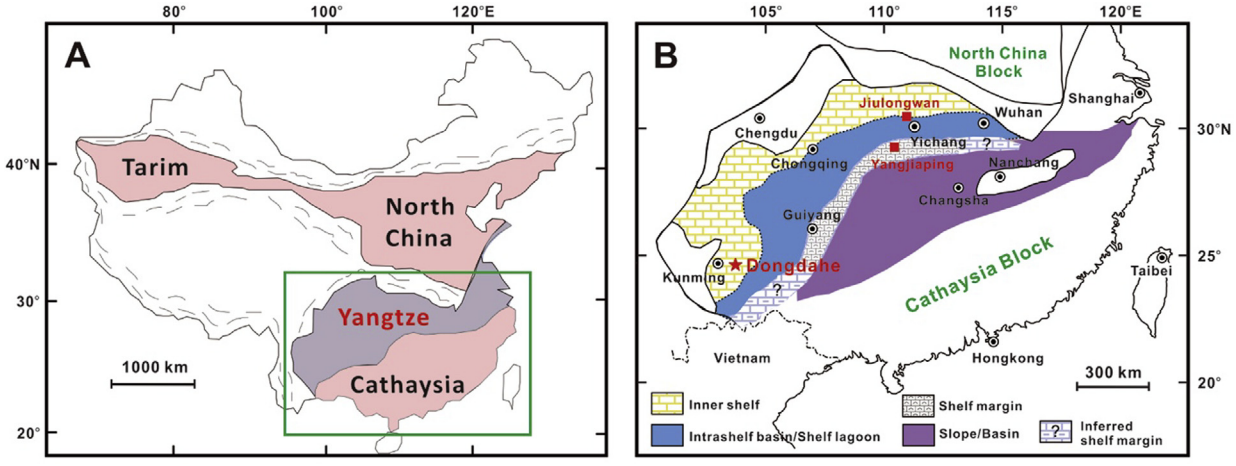

Fig. 1. (A) Major tectonic blocks of China. (B) Geologic location of the Dongdahe section and the Ediacaran paleogeographic map of the Yangtze carbonate platform in South China (modified from Jiang et al., 2011).

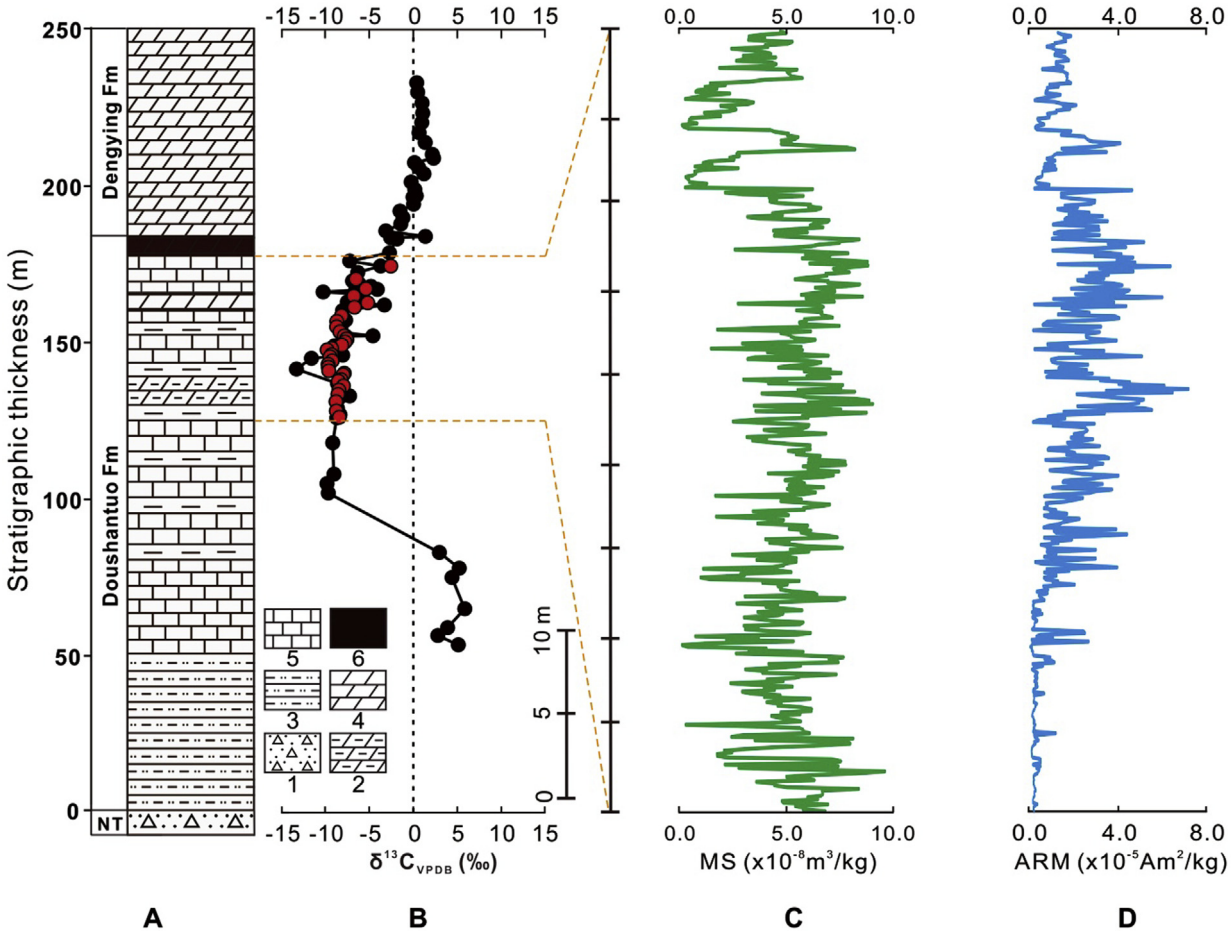

Fig. 2. Stratigraphic column, carbon isotope stratigraphy and rock magnetic cyclostratigraphies. (A) Stratigraphic column of the Dongdahe section. (B) Carbon isotope profiles. Black circles are data from Zhu et al. (2007), red circles are data from this study. (C) 45-m raw MS series. (D) 45-m raw ARM series. Legends for stratigraphic column are: (1) diamictite; (2) muddy dolostone; (3) sandstone; (4) dolostone; (5) limestone; (6) black shale.

that the folding was of mid-Cenozoic in age and probably resulted from the Indo-Asian collision (Liang et al., 1984).

3. Methods

3.1. Sampling and preparation

In order to observe a full suite of Milankovitch frequencies in spectral analysis, we must use a sampling interval that would detect precession, which is the shortest Milankovitch cycle. Theoretical estimates indicate that the longest precession period at 500–550 Ma is of 20.5 kyr (Berger and Loutre, 1994; Waltham, 2015), therefore we need to collect samples at least every 10.3 kyr (Nyquist frequency). The average thickness of the bedding in the Doushantuo carbonates is ~10 cm. We chose a 10 cm sampling interval for rock magnetic cyclostratigraphy, which means that our Nyquist frequency is 1/20 cm^{-1}. As long as the sediment accumulation rate of the Doushantuo Formation is no less than 1.0 cm/kyr, the sampling interval we chose should be sufficient to reveal all Milankovitch cycles in spectral analysis. In the field, the 8-m black shale (Doushantuo Member IV) was used as a stratigraphic marker in order to compare our section to the chemostratigraphic section of Zhu et al. (2007). Because no samples were collected from the black shale, our samples covered 45 m of the Doushantuo Member III. A total of 450 unoriented samples were collected for rock magnetic cyclostratigraphy. Unoriented samples were cut using a drill press and a diamond bladed saw to yield mini-cores in a uniform size (1.5 cm in length, 1.0 cm in diameter) at Lehigh University. Using a portable gasoline-powered drill, we collected oriented samples from 24 sites for paleomagnetic measurements at a stratigraphic sampling interval of 2–3 m. Each site consists of at least 3 oriented samples. These samples were trimmed to yield 101 standard size paleomagnetic cores (2.2 cm in length, 2.5 cm in diameter) in total. Rock chips left over from preparation of the unoriented cyclostratigraphic samples were trimmed to remove any weathered surfaces for rock magnetic, carbon isotopic and scanning electron microscopic (SEM) analyses.

3.2. Magnetic measurements

Stepwise demagnetization of the oriented cores was conducted in a magnetostatically-shielded room (ambient field intensity <350 nT) in the Paleomagnetism Laboratory at Lehigh University. Thermal demagnetization was conducted typically from 100 °C to 580 °C in 20 steps using an ASC Model TD-48SC thermal demagnetizer. Remanence was measured by a 2G Enterprises 755 superconducting rock magnetometer. Alternating-field (AF) demagnetization was conducted on sister cores in 5 mT intervals from 5 mT to 110 mT using an AF demagnetizer built into the 2G superconducting magnetometer. Cores in which the remanence was not completely demagnetized by the AF technique were further thermally demagnetized in 3 steps from 150 °C to 200 °C. Vector-endpoint diagrams (Zijderveld, 1967) were plotted and the characteristic remanent magnetization (ChRM) of each core

was determined by principal component analysis (PCA; Kirschvink, 1980). Paleomagnetic data were analyzed in the PuffinPlot (Lurcock and Wilson, 2012). Fisher statistics was used to calculate mean paleomagnetic directions using the Stereonet (Cardozo and Allmendinger, 2013).

Rock magnetic experiments were performed on 8 representative samples for magnetic mineralogy identification. The partial anhysteretic remanent magnetization (pARM) measurements were conducted using a modified Schonstedt GSD-5 AF demagnetizer with a steady biasing DC field of 97 μT to study the magnetic grain size distribution (Jackson et al., 1988). We performed stepwise isothermal remanent magnetization (IRM) acquisition from 0 T to 1.2 T in 22 steps with an ASC impulse magnetizer and used modeling (Kruiver et al., 2001) to resolve the magnetic coercivity components and their contributions to the saturation isothermal remanent magnetization (SIRM). Lowrie test was employed by thermally demagnetizing three orthogonal IRMs applied in fields of 1.2 T, 0.6 T and 0.1 T (Lowrie, 1990). The temperature dependence of magnetic susceptibility was measured from 20 °C to 700 °C in an argon gas environment. The magnetic susceptibility (MS) of a total of 450 unoriented samples was measured with an Agico Kappabridge KLY-3S susceptibility meter. The anhysteretic remanent magnetization (ARM) of each unoriented sample was applied in a 100 mT peak AF window (biasing DC field 97 μT). MS and ARM values of each sample were measured three times for a reproducibility check and normalized by sample mass. Raw MS and ARM series are shown in Fig. 2C and D.

3.3. Spectral analysis

Spectral analysis was conducted using the Analyseries (Paillard, 1996). Both MS and ARM series were evenly resampled at a 10 cm interval using linear interpolation. The power of long wavelength cycles (>45 m) in the MS and ARM series were removed by a Gaussian notch filter. Notch-filtered MS and ARM series are shown in Fig. 3. The multi-taper method (MTM; Thomson, 1982) with 2π prolate multi-tapers was used (Ghil et al., 2002) for spectral analysis. Robust red noise (Mann and Lees, 1996) and the confidence levels of 90%, 95% and 99% above the robust red noise were calculated to determine significant spectral peaks. In order to test the presence of Milankovitch cycles, ratios of the frequencies of significant spectral peaks were calculated and compared to the ratios of predicted frequencies of orbital cycles at 500–550 Ma (Berger and Loutre, 1994; Waltham, 2015). Because the long eccentricity is the most stable Milankovitch cycle throughout geologic history and has the least uncertainty in its period (Laskar et al., 2011), we use it to calculate the sediment accumulation rate of the Doushantuo Formation at the Dongdahe section. The duration of the SE is then determined from the stratigraphic thickness of the SE and the calculated sediment accumulation rate at the Dongdahe section. Because eccentricity variations modulate the amplitude of precession cycles (Weedon, 2003), amplitude modulation analysis (Hinnov, 2000) was conducted. The MS and ARM series were filtered at the wavelength of the spectral peak identified to be precession and the envelopes of the precession-filtered MS and ARM series were analyzed for eccentricity cyclicities using MTM spectral analysis.

3.4. Carbon isotopic analysis

The lowest part of the Dongdahe section is exposed in a cliff so we did not obtain a record of the entire SE, making our own carbon isotopic measurements important for precisely locating the stratigraphic positions of our samples with respect to the previous carbon isotopic study (Zhu et al., 2007) and determining the part of the SE that we sampled. Representative whole-rock samples were rinsed with distilled water and crushed into homogeneous powder. Around 350 μg of each sample was reacted with 100% H_3PO_4 at 70 °C for at least 2 hours in the presence of He gas and then measured with a Finnigan MAT252 mass spectrometer interfaced with a Gas Bench II in the Stable Isotope Geochemistry Laboratory at Lehigh University. Regular analysis of a house standard and the international standard NBS19 calcite allows monitoring and correction of the data, resulting in a standard deviation (1σ) of ~0.2‰ for $\delta^{13}C$. The $\delta^{13}C$ values are reported relative to the Vienna Pee Dee Belemnite (VPDB).

3.5. SEM analysis

Representative samples were ground into powder by a mortar and a pestle and mixed with distilled water to create a slurry. The slurry was circulated past a magnetic needle for one week to extract the magnetic particles (Hounslow and Maher, 1999). SEM analysis was undertaken to assess the morphology, size and chemical composition of the extracted magnetic particles using a Hitachi TM-1000 tabletop SEM operating at 15 keV and an

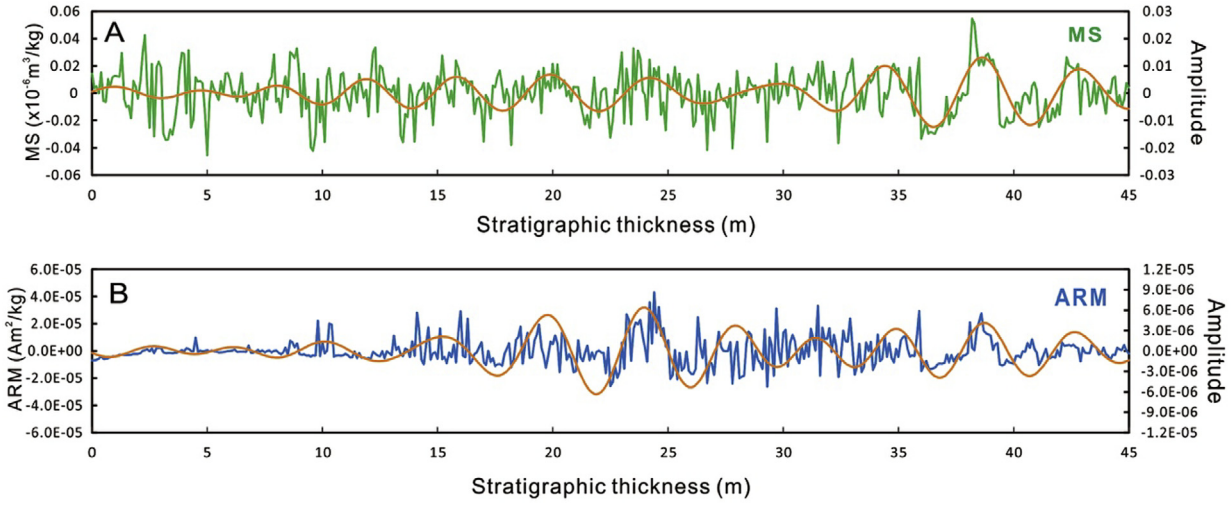

Fig. 3. The MS and ARM series are filtered by a Gaussian notch filter to remove the power of long wavelength cycles (>45 m). Orange lines are the MS and ARM series filtered at the interpreted long eccentricity wavelength.

Energy-Dispersive Spectrometer (EDS) with a Silicon Drift Detector (SDD) at Lehigh University. The SDD has a Be window allowing EDS analysis of elements heavier than Na.

4. Results

4.1. Paleomagnetism

The natural remanent magnetization (NRM) intensities of our samples are less than 1.0 mA/m, which are typical values for carbonate rocks. Both AF (Fig. 4A) and thermal (Fig. 4B) demagnetizations yield consistent results. Most cores (88%) have two component magnetizations (Fig. 4). Component 1 is aligned with the present-day geomagnetic field of the Dongdahe section and is easily removed by heating at 150 °C or by an AF at 10 mT, matching remanence expectations for either secondary goethite or a viscous overprint carried by large magnetic grains. Component 2 demagnetizes univectorially towards the origin on a vector-endpoint diagram and unblocks above 500 °C, which is defined as the ChRM of each core. All ChRMs show a single polarity. Because the folding of the Dongdahe section was mid-Cenozoic, we applied a tilt correction to all ChRMs (Fig. 5). The mean ChRM of the Doushantuo Formation from the Dongdahe section is $D_s = 19.1°$, $I_s = 36.5°$ ($\alpha_{95} = 2.8°$, k = 120.6; Fig. 5) and its corresponding paleomagnetic pole is located at 71.8°N, 203.1°E ($A_{95} = 2.5°$, Fig. 6).

4.2. Magnetic mineralogy

IRM acquisition experiments of representative samples show that most samples are fully saturated by 0.6 T while a few samples are not completely saturated by 1.2 T (Fig. 7). IRM modeling indicates that the acquisition curve can be best fit by two coercivity components, a soft component with the mean coercivity lower than 65 mT and a hard component with the mean coercivity higher than 1.5 T (Fig. 7; Table 1). Lowrie test shows that the remanence of the hard component can be easily removed by 100 °C (Fig. 8A). Based on its high coercivity (0.6–1.2 T) and low unblocking temperature (~100 °C), the hard component is probably goethite. The soft component largely unblocks by 500–550 °C (Fig. 8), which is close to the Curie temperature of titanomagnetite.

The results of susceptibility-temperature experiments also support the presence of titanomagnetite. Representative susceptibility-temperature (K-T) curves show a sharp decrease of magnetic susceptibility at 500–560 °C during heating. A Hopkinson peak appears at temperatures immediately below the Curie temperature on a heating curve (Fig. 9B). An increase of magnetic susceptibility was also noticed on cooling curves (Fig. 9A), indicating new ferromagnetic minerals were produced during heating.

The pARM experiment indicates a uniform size distribution for the titanomagnetite detected in our samples. The peak of the pARM intensities lies in 15–20 mT range (Fig. 10), implying that the mean size of titanomagnetite grains is about 5 μm (Jackson et al., 1988). This grain size is larger than the single domain (SD) threshold for titanomagnetite (Butler and Banerjee, 1975). Therefore, the titanomagnetite grains in our samples are probably pseudo-single domain (PSD) or small multidomain (MD) in size.

4.3. Spectral analysis

MTM spectral analysis of the MS series of the Doushantuo Formation shows a suite of significant spectral peaks that rise above the 95% confidence level at wavelengths of 427 cm, 85 cm, 30.4 cm, 27.3 cm, 21.9 cm and 20.7 cm (Fig. 11A; Table 2). MTM spectral analysis of the ARM series of the Doushantuo Formation yields significant spectral peaks at similar wavelengths of 410 cm, 136 cm, 29.2 cm, 27.8 cm, 25.8 cm and 22.1 cm (Fig. 11B; Table 2). The wavelengths of significant spectral peaks obtained from the MS and ARM series are not exactly identical, but given the uncertainties in their wavelengths (half bandwidth of the spectral peak; Weedon, 2003), two spectra reveal consistent significant spectral peaks at ~420 cm, ~100 cm, ~28 cm and ~22 cm.

In the amplitude modulation analysis, MTM spectral analysis of the envelope of the precession-filtered MS series reveals spectral peaks at wavelengths of 2048 cm, 640 cm, 427 cm, 256 cm, 116 cm, 99 cm and 76 cm (Fig. 12A and C). The spectral analysis of the envelope of the precession-filtered ARM series reveals spectral peaks at wavelengths of 2048 cm, 602 cm, 445 cm, 233 cm, 107 cm, 89 cm and 80 cm (Fig. 12B and D).

4.4. Carbon isotopic analysis

The base of the upper Dongdahe section has a $\delta^{13}C_{VPDB}$ value of −8.4‰. $\delta^{13}C_{VPDB}$ values decrease upsection to the lowest value of −9.8‰ that is 23.5 m below the base of the black shale (Doushantuo Member IV), and gradually increase upsection to −1.8‰ at the base of the black shale. Our carbon isotope profile agrees well with that of Zhu et al. (2007; Fig 2B). Based on stratigraphic and carbon isotope correlations with published data, the 45-m Dongdahe section we sampled records 50 ± 5% of the SE.

4.5. SEM analysis

The SEM search for magnetic grains focused on identification of grains showing significant Fe peaks in the EDS spectra. Sulfur was not observed in the EDS spectra of the Fe-rich grains, suggesting that our samples are dominated by iron oxides rather than iron sulfides (Fig. 13B and C). In combination with the evidence from rock magnetic experiments, we interpret the Fe oxides to be titanomagnetite. The titanomagnetite grains are angular and irregular in shape, and about ~5 μm in size (Fig. 13A). This grain size agrees well with the results of pARM experiments and suggests that we were able to magnetically separate the dominant grain size of titanomagnetite in our samples. We also detected Si, Al and Ca in the EDS spectra due to the clay minerals and carbonates adhered to the surface of titanomagnetite grains that were not completely removed (Fig. 13C).

5. Discussion

5.1. Paleomagnetism of the Doushantuo Formation

Previous paleomagnetic studies of the Doushantuo Formation in South China show two distinct remanence directions. A shallow and single polarity remanence was obtained from the Yangjiaping section in northwestern Hunan Province (Macouin et al., 2004; Figs. 1B and 5). In contrast, a recent study from the Jiulongwan section in western Hubei Province provides a steeper and dual polarity remanence (Zhang et al., 2015; Figs. 1B and 5). These two sections, although having slight mismatches in stratigraphic thickness and carbon isotope values due to different depositional settings on the Yangtze carbonate platform, can be stratigraphically correlated to the Dongdahe section (Zhu et al., 2007; Jiang et al., 2007). The SE with the nadir $\delta^{13}C$ value of ~−10‰ has been consistently observed in Doushantuo Member III from all the three sections in South China (Zhu et al., 2007; Jiang et al., 2007).

The mean ChRM and the corresponding paleomagnetic pole from the Dongdahe section are distinct from the results of two previous studies (Figs. 5 and 6). Because the stratigraphic positions of the three studies are slightly different (the Yangjiaping samples are from Doushantuo Members II and III, our samples are from upper

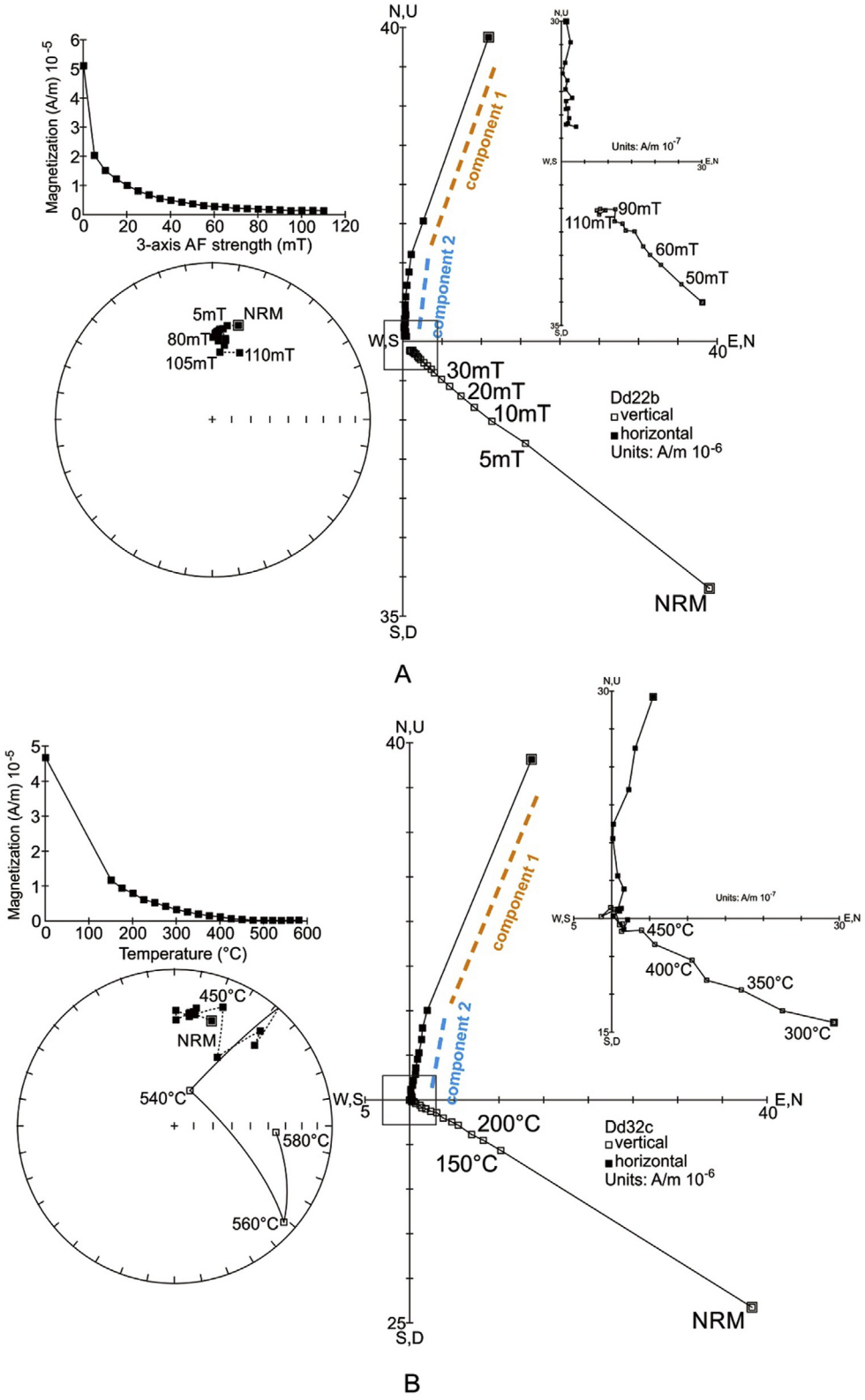

Fig. 4. Vector-endpoint diagrams of demagnetization data (Zijderveld, 1967; stratigraphic coordinates). Representative trajectories of (A) alternating-field and (B) thermal demagnetizations. Open and solid squares are vertical and horizontal vectors, respectively. Orange and blue dash lines indicate two magnetization components. (For interpretation of the references to colour in this figure legend, the reader is referred to the web version of this article.)

Doushantuo Member III, and Jiulongwan samples are from the top 8-m of the Doushantuo Member III), samples from the three sections may not be exactly the same age. Therefore, it is theoretically possible that all three remanences could be primary. The Dongdahe samples are stratigraphically very close to the Jiulongwan samples. Assuming that both the Jiulongwan and Dongdahe paleopoles are

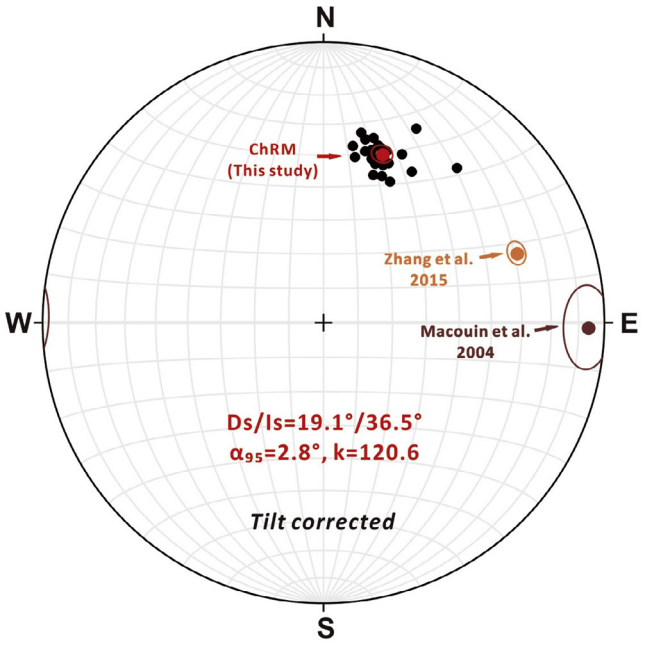

Fig. 5. Equal area stereography of paleomagnetic results from the Doushantuo Formation in stratigraphic coordinates. Black circles indicate the 24 ChRM site means, red circle is the mean of the site means for this study, brown circle is the mean ChRM direction from Macouin et al. (2004) and orange circle is the mean ChRM direction from Zhang et al. (2015). The corresponding 95% confidence cones are shown using the same color code. (For interpretation of the references to colour in this figure legend, the reader is referred to the web version of this article.)

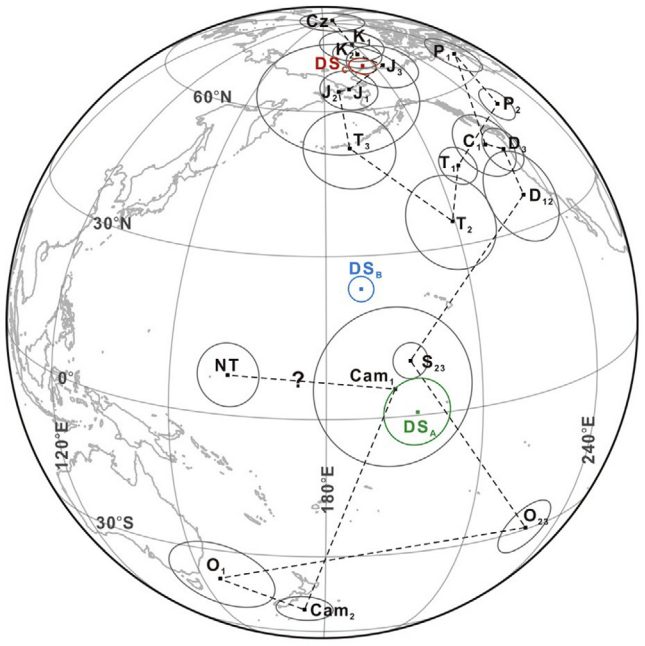

Fig. 6. Stereographic projection of Neoproterozoic and Phanerozoic paleomagnetic poles for South China. Paleopoles are those synthesized in Table 2 of Zhang et al. (2015). Plot was made by the GPlates (Boyden et al., 2011). DS_A is the Yangjiaping paleopole from Macouin et al. (2004), DS_B is the Jiulongwan paleopole from Zhang et al. (2015) and DS_C is the paleopole of this study. NT is Cryogenian Nantuo Formation, Cam is Cambrian, O is Ordovician, S is Silurian, D is Devonian, C is Carboniferous, P is Permian, T is Triassic, J is Jurassic, K is Cretaceous, Cz is Cenozoic. Subscripts 1, 2, 3 mean early, middle and late, respectively.

primary would indicate a rapid and large apparent polar wander path (APWP) excursion for South China in the Ediacaran, analogous to that observed for the Ediacaran paleopoles from Laurentia and Baltica (Abrajevitch and Van der Voo, 2010). But the Dongdahe paleopole is very close to the late Jurassic and Cretaceous paleopoles for South China (Huang et al., 2008; Fig. 6). In addition, all the ChRMs from the Dongdahe samples have a single polarity and no field test is available for a paleomagnetic stability check. Therefore, it is very likely that the Dongdahe samples carry a late Mesozoic remagnetization. The Yangjiaping paleopole is also suspicious because it is very close to the early Cambrian and Silurian paleopoles for South China (Zhang et al., 2015; Fig. 6). Even though the age of the remanence from the Yangjiaping section is supported to be pre-Jurassic by a positive fold test, an early Paleozoic remagnetization is still possible (Zhang et al., 2015). The Jiulongwan paleopole is the only result from the Doushantuo Formation that passes the reversal test and is most likely primary (Zhang et al., 2015; Fig. 6). But a trend of steepening inclinations upsection in their group 1 samples (Fig. 2 in Zhang et al., 2015) could possibly indicate a secondary remanence that has not been adequately removed (Jing et al., 2015). Additional studies are needed to constrain the uncertainties of the magnetostratigraphy and paleogeography of the Doushantuo Formation.

Because we suspect that a late Mesozoic remagnetization affected the Dongdahe samples, a magnetic mineralogy study is important to understand the possible remagnetization mechanism and the validity of the rock magnetic cyclostratigraphy. Rock magnetic experiments clearly show the presence of goethite and titanomagnetite. Goethite was probably formed by recent weathering since its remanence is parallel to the present-day geomagnetic field direction of the Dongdahe section. The remanence carried by goethite is completely removed by the thermal demagnetization at 150 °C, so goethite does not contribute to the ChRM. The ChRM is carried by titanomagnetite. Careful SEM analysis shows that the shape of the titanomagnetite is angular and irregular, suggesting that they are detrital grains and have not been affected by chemical dissolution. There is also no observation of botryoidal, spheroidal or euhedral authigenic grains suggesting diagenesis and the acquisition of a chemical remanent magnetization (CRM; McCabe et al., 1983; Suk et al., 1990; Zhang et al., 2016; Fig. 13). If the ChRMs of the Dongdahe samples record a remagnetization, it more likely has resulted from a thermoviscous remanent magnetization (TVRM). Because all ChRMs are single polarity and its corresponding paleopole is close to the late Mesozoic paleopole of South China, we speculate that a stable TVRM may have been acquired during the Cretaceous normal polarity superchron when PSD or small MD titanomagnetite grains in the Dongdahe samples experienced a prolonged episode of heating during the late Mesozoic Yanshanian orogeny. But this contention is not definitive. Further investigations are required. Even though the Dongdahe samples probably carry a late Mesozoic overprint, at least, the detrital titanomagnetite grains are dominant in the samples and carry a primary, orbitally-forced cyclostratigraphy in the Ediacaran.

5.2. Duration of the SE

MTM spectral analysis of the MS and ARM series reveals significant spectral peaks at similar frequencies (Fig. 11). To identify the presence of Milankovitch cycles in spectral analysis, we used Laskar et al. (2004)'s model for the expected periods of the long and short eccentricities. The Berger and Loutre (1994)'s model was used for the predicted periods of obliquity and precession at 500 Ma. A newly developed model by Waltham (2015) was also used because it calculates the predicted periods of obliquity and precession at 550 Ma, closer to the SE in age.

The initial estimate of the sediment accumulation rate of the Doushantuo Formation is of 0.2 cm/kyr based on its 84 Myr duration and its 180 m stratigraphic thickness at the Dongdahe section

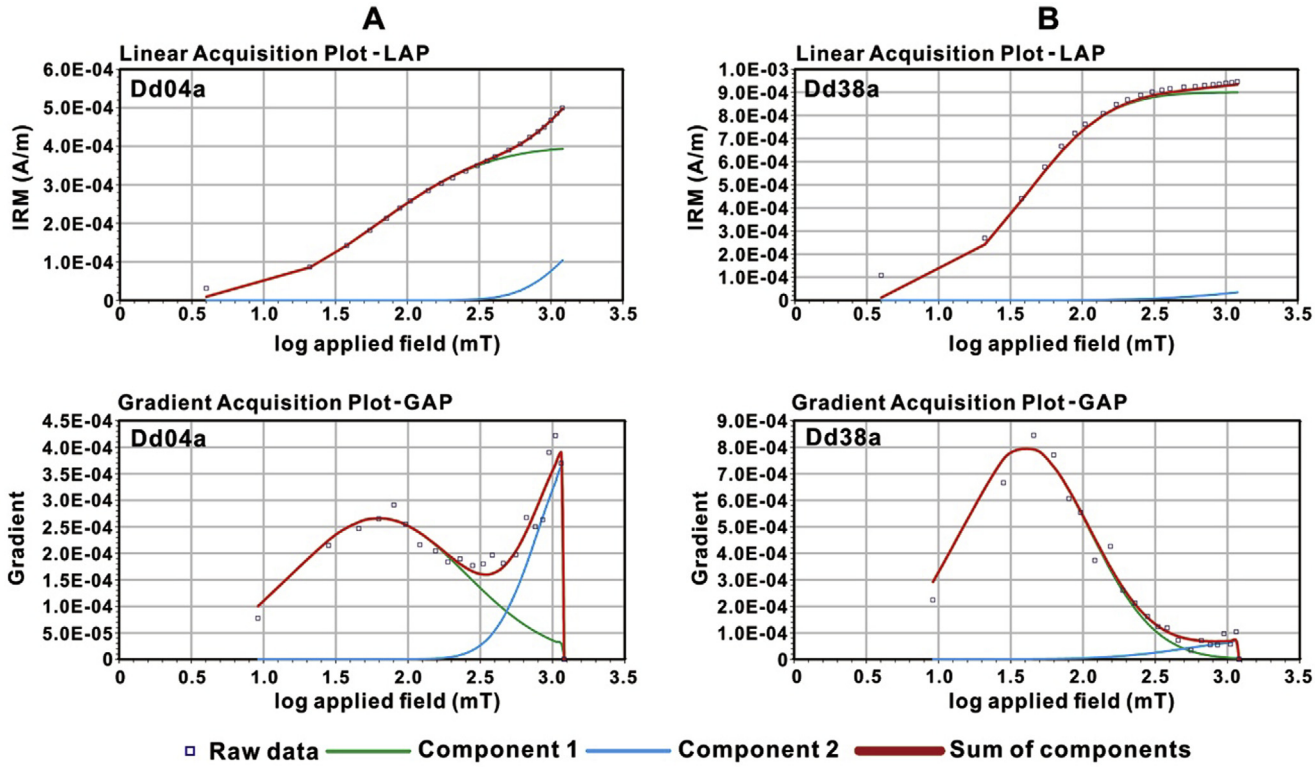

Fig. 7. Modeling of coercivity components observed in IRM acquisition experiments (Kruiver et al., 2001). The IRM acquisition data are best fit by two coercivity components. Detailed information about each coercivity component is shown in Table 1.

Table 1
Results of the IRM acquisition modeling. $B_{1/2}$ is the mean coercivity, DP is the half-width of the distribution.

	Component	Contribution (%)	SIRM (A/m)	log $B_{1/2}$ (mT)	$B_{1/2}$ (mT)	DP (mT)
Dd04a	1	57.1	4.0E−04	1.8	63.1	0.60
	2	42.9	3.0E−04	3.2	1584.9	0.30
Dd38a	1	90.0	9.0E−04	1.6	39.8	0.45
	2	10.0	1.0E−04	3.3	1995.3	0.55

(Knoll et al., 2006; Zhu et al., 2007). But this rate is an underestimate because of unconformities identified at the base and the top of the Doushantuo Formation (Jiang et al., 2011). When we set the ~420 cm spectral peak to long eccentricity, the ratios of the frequencies of other spectral peaks for a given rock magnetic series agree well with the ratios of predicted Milankovitch periods at 500–550 Ma (Laskar et al., 2004; Berger and Loutre, 1994; Waltham, 2015; Table 2). Specifically, in the MS spectrum, if the 427 cm spectral peak is set to long eccentricity, then the 85 cm spectral peak is 80.7 kyr in duration (close to short eccentricity), the spectral peaks at 30.4 cm and 27.3 cm are 28.9 kyr and 25.9 kyr in duration (close to obliquity), and the spectral peaks at 21.9 cm and 20.7 cm are 20.8 kyr and 19.7 kyr in duration (close to precession). In the ARM spectrum, if the 410 cm spectral peak is set to long eccentricity, then the spectral peak at 136 cm is 134.5 kyr in duration (chose to short eccentricity), the spectral peaks at 29.2 cm, 27.8 cm and 25.8 cm are 28.9 kyr, 27.5 kyr and 25.5 kyr in duration (close to obliquity), and the spectral peak at 22.1 cm is 21.9 kyr in duration (close to precession). We note that the ratios of the frequencies of the significant spectral peaks have slight misfits compared to the ratios predicted from the two models, especially for precession (Table 2). This is reasonable because precession has larger uncertainties in its period back in time than other Milankovitch cycles (Laskar et al., 2011). Waltham (2015)'s model better matches the obliquity and precession in the MS and ARM series since it provides predicted periods for the Milankovitch cycles at 550 Ma, closer to the age of the SE, compared to the Berger and Loutre (1994)'s model that only predicts orbital periods at 500 Ma. In addition, the calculation of periods of obliquity and precession by Waltham (2015)'s model has considered the change in lunar-recession rate, which is assumed to be constant by Berger and Loutre (1994). Therefore, Waltham (2015)'s model should provide more accurate Milankovitch periods in the Ediacaran.

We filtered the MS and ARM series at 427 cm and 410 cm wavelengths (interpreted to be long eccentricity) and superimposed them on the notch-filtered series (Fig. 3). The eccentricity-filtered MS and ARM series correlate with the first order oscillations of the data series, indicating the consistency of the power of the ~420 cm spectral peak throughout the 45 m Doushantuo Member III. Spectral analysis of the envelopes of the precession-filtered MS and ARM series clearly shows that the amplitude of precession is modulated by several cycles (Fig. 12). The spectral peak at ~2050 cm may represent the 2.4 Myr cycle of long-term variations in eccentricity (Weedon, 2003). Spectral peaks at ~430 cm, ~110 cm and ~94 cm correspond to long (405.6 kyr) and short eccentricities (123.9 kyr and 94.9 kyr). Although spectral peaks at other wavelengths are also observed and are difficult to interpret, amplitude modulation analysis shows that the spectral peak

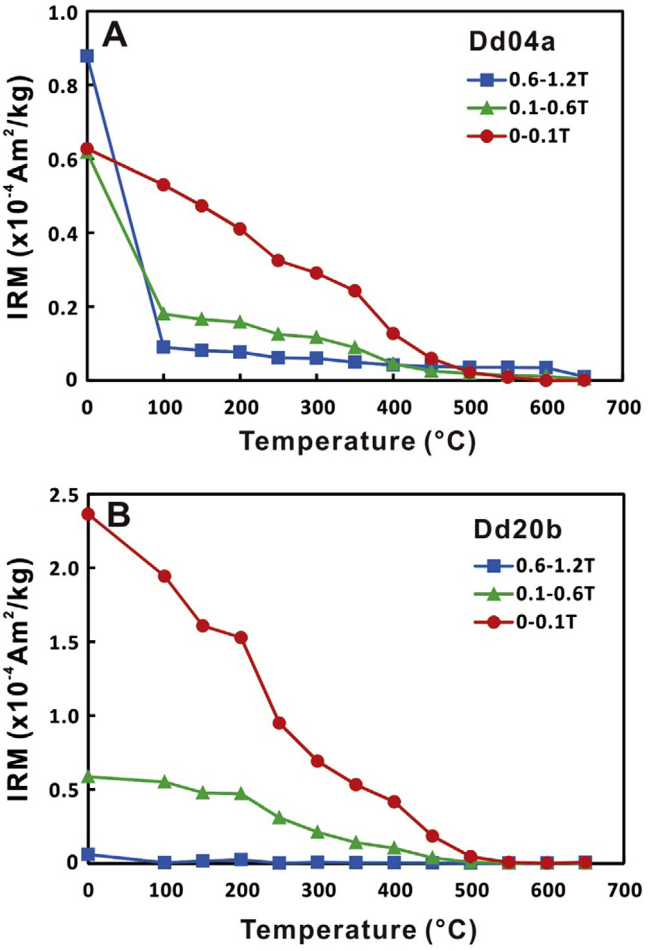

Fig. 8. Representative thermal demagnetization of IRMs applied in three coercivity ranges (0–0.1 T; 0.1–0.6 T; 0.6–1.2 T). Lowrie test (Lowrie, 1990) shows that the high coercivity component mostly unblocks by 100 °C.

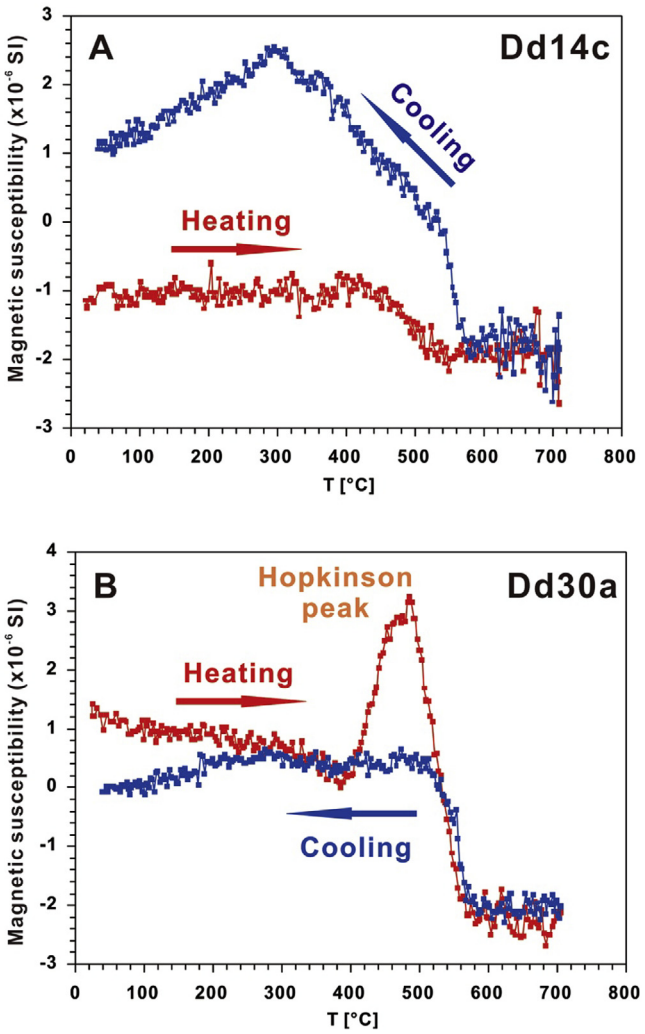

Fig. 9. Susceptibility versus temperature results. (A) A significant decrease of magnetic susceptibility is noticed between 500–560 °C. (B) The Hopkinson peak appears immediately below the Curie temperature.

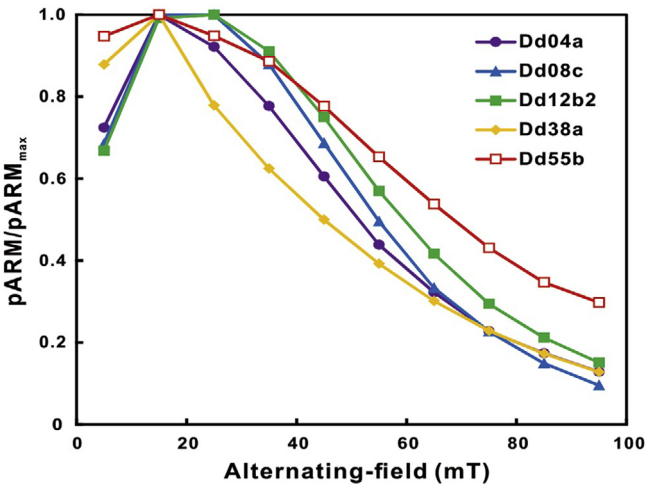

Fig. 10. Partial ARMs show that the peak intensities occur at ~20 mT, suggesting a mean grain size of ~5 μm for titanomagnetite.

interpreted to be precession is modulated by eccentricity, further supporting that the significant spectral peaks in the MS and ARM series are orbital in origin (Fig. 12).

Since the cycles in the MS and ARM series are identified to be Milankovitch cycles, we use the average wavelength of long eccentricity peak in our data and the period of long eccentricity in the Ediacaran (405.6 kyr; Laskar et al., 2004), and calculate the sediment accumulation rate of the Doushantuo Formation at the Dongdahe section to be 1.0 cm/kyr. This low rate, although not commonly observed in modern carbonate platform environments, agrees reasonably well with the initial estimate based on geochronologic data. Low sediment accumulation rates of the same magnitude have been reported from the Devonian St. George Group in western Newfoundland and the Triassic Trogkofel Formation in Southern Alps (synthesized by Bosscher and Schlager, 1993).

The cyclicities observed in the MS and ARM series of the Doushantuo Formation suggest that global orbitally-forced climate cycles were encoded by the concentration variations of detrital titanomagnetite. The same encoding mechanism has also been observed from the Eocene Arguis Formation in Spanish Pyrenees (Kodama et al., 2010) and the Triassic Daye Formation in South China (Wu et al., 2012). Considering the low-latitude position of the Yangtze carbonate platform in the Ediacaran (Li et al., 2008; Zhang et al., 2015), it is possible that monsoon intensity variations driven by orbitally-forced insolation controlled the amount of terrestrial siliciclastics delivered into a background of relatively constant marine carbonate production.

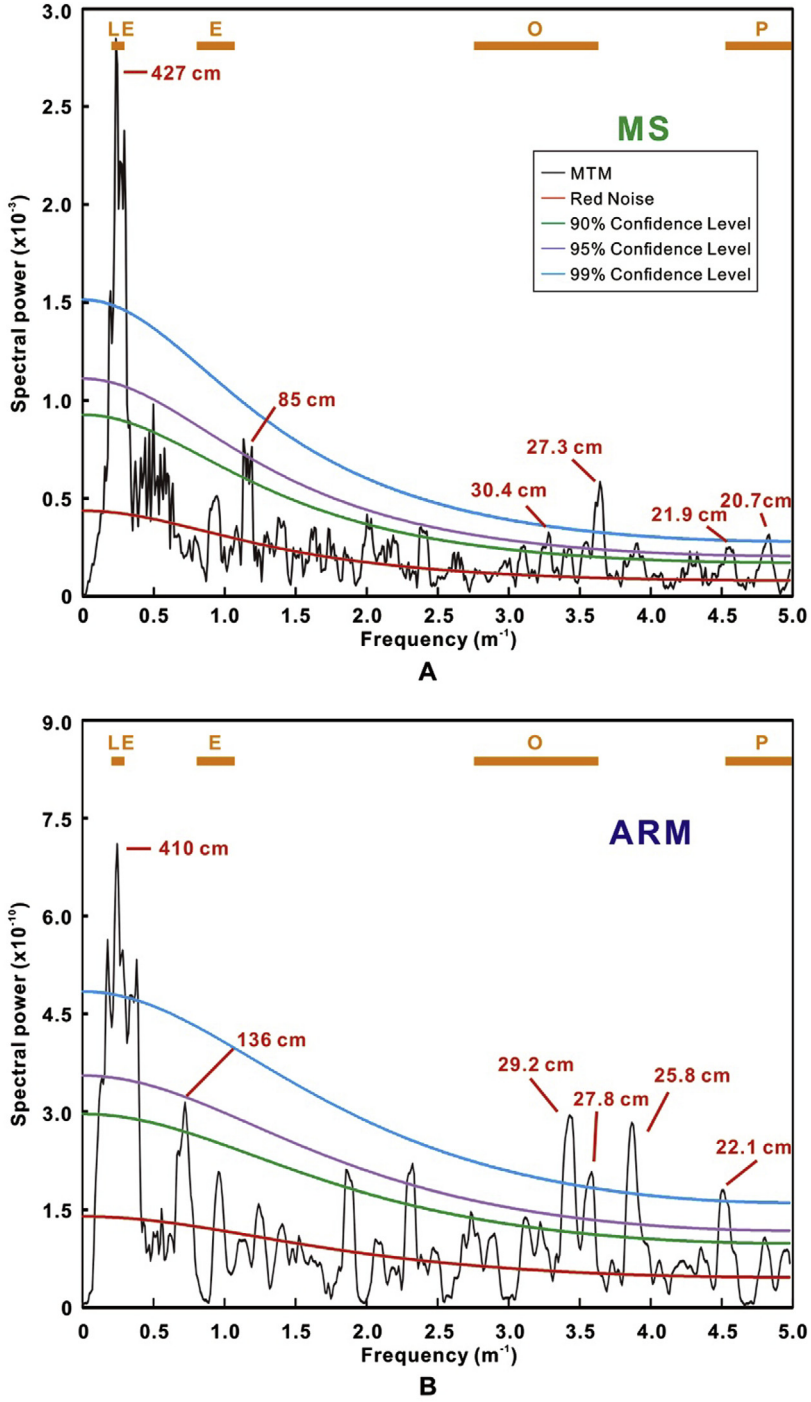

Fig. 11. MTM spectral analysis of (A) the MS and (B) the ARM series. Wavelengths of significant spectral peaks are shown in red numbers. The robust red noise is represented by the red line. The 90%, 95% and 99% confidence levels above the robust red noise are indicated by green, purple and blue lines, respectively. Orange bands show the predicted frequency range for long eccentricity (LE), short eccentricity (E), obliquity (O) and precession (P) at 500–550 Ma (Laskar et al., 2004; Waltham, 2015). (For interpretation of the references to colour in this figure legend, the reader is referred to the web version of this article.)

Kodama and Hinnov (2014) point out that misidentification of Milankovitch cycles could occur if the ratio of orbital cycles is the only basis for identification without other age constraints. This issue is also thoroughly discussed by Waltham (2015). The least robust interpretation results from using the ratio of only two Milankovitch cycles for spectral peak identification. The improvement of our study compared to Minguez et al. (2015) regarding spectral peak identification is that instead of using the ratio of only two Milankovitch cycles, we use the ratios of a suite of Milankovitch cycles (long eccentricity, short eccentricity, obliquity and precession), which effectively reduces the possibility of misidentification. The amplitude modulation analysis further reinforces our interpretation.

Using the 1.0 cm/kyr sediment accumulation rate obtained from rock magnetic cyclostratigraphy, we estimate that the duration of the 45-m Doushantuo Member III was deposited over a duration of 4.5 Myr. Because the lithology and depositional environment are fairly invariant at the Dongdahe section, if this

Table 2
Results of the MTM spectral analysis. Predicted Milankovitch periods match to the wavelengths of significant spectral peaks resolved from the MS and ARM series in the Doushantuo Formation. Ratio calculation uses the predicted Milankovitch frequencies and the frequencies of significant spectral peaks in the MS and ARM series. Periods of the long and short eccentricities are from Laskar et al. (2004). Periods of the obliquity and the precession are from Berger and Loutre (1994) and Waltham (2015), respectively. LE is long eccentricity, E is short eccentricity, O is obliquity and P is precession.

Doushantuo cyclicity						Astronomical cyclicity				
MS			ARM			Berger and Loutre (1994)		Waltham (2015)		Milankovitch cycles
Wavelength (cm)	Chronology (kyr)	Ratio	Wavelength (cm)	Chronology (kyr)	Ratio	Period (kyr)	Ratio	Period (kyr)	Ratio	
427	405.6	1	410	405.6	1	405.6	1	405.6	1	LE
–	–	–	136	134.5	3.0	123.9	3.3	123.9	3.3	E
85	80.7	5.0	–	–	–	94.9	4.3	94.9	4.3	
30.4; 27.3	28.9; 25.9	14.8	29.2; 27.8; 25.8	28.9; 27.5; 25.5	14.9	36.2–29.9	11.2–13.7	36.2–27.6	11.2–14.7	O
21.9; 20.7	20.8; 19.7	20.0	22.1	21.9	18.5	19.0–16.2	21.3–25.0	22.0–15.5	18.4–26.1	P

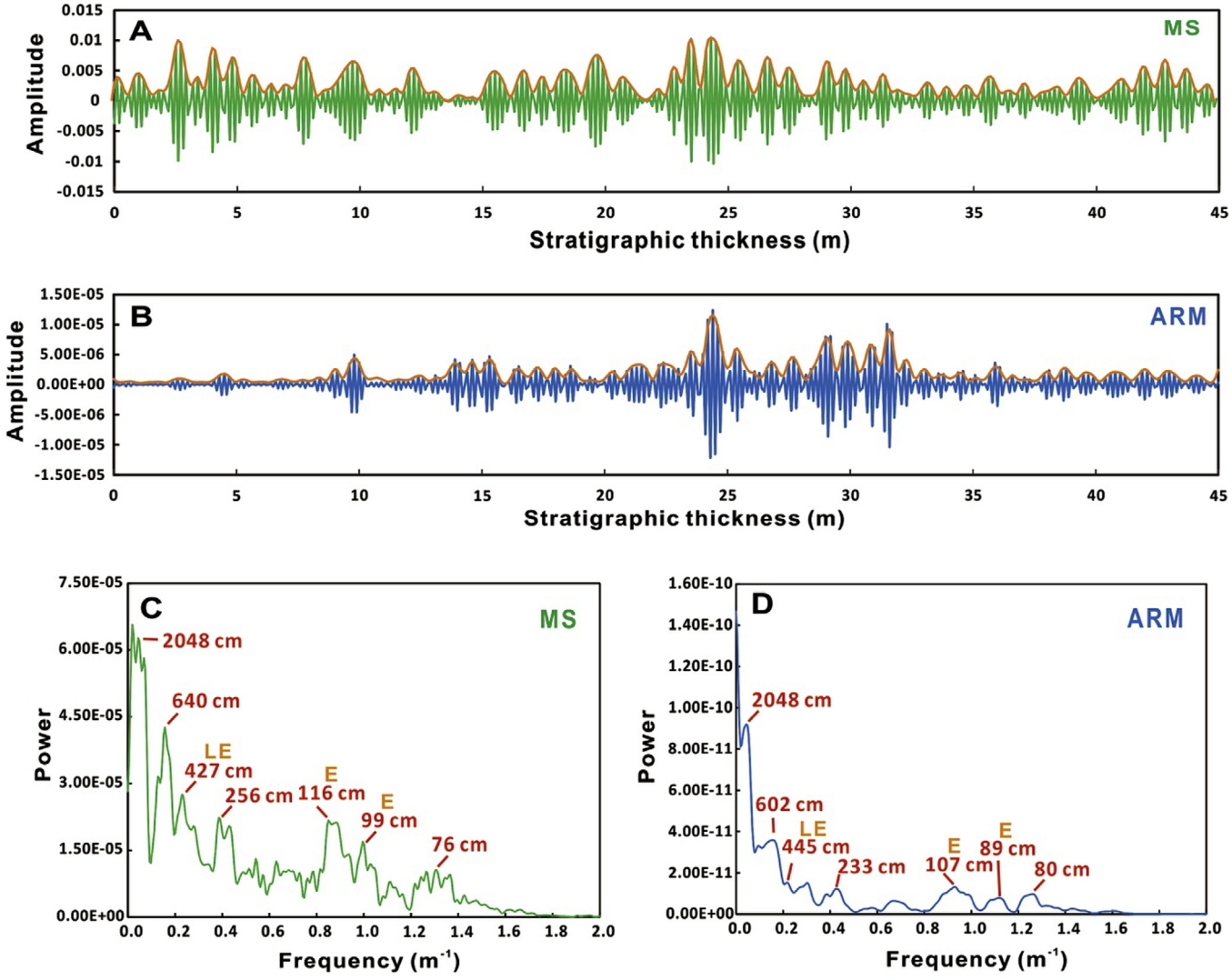

Fig. 12. Amplitude modulation analysis. (A) MS series is filtered at the interpreted precession wavelength. (B) ARM series is filtered at the interpreted precession wavelength. (C) Power spectrum of envelope of precession-filtered MS series. (D) Power spectrum of envelope of precession-filtered ARM series. Orange lines are the envelopes. Red numbers indicate the wavelengths of peaks revealed in the MTM spectral analysis of the envelope. LE is long eccentricity and E is short eccentricity. (For interpretation of the references to colour in this figure legend, the reader is referred to the web version of this article.)

sediment accumulation rate is assumed to have remained constant, the entire SE in South China is estimated to be 9.1 ± 1.0 Myr in duration. Our estimate agrees, within uncertainty, with the results for the Johnnie Formation of the Death Valley region, North America (8.2 ± 1.2 Myr; Minguez et al., 2015), and the Wonoka Formation, South Australia (8.0 ± 0.5 Myr; Minguez

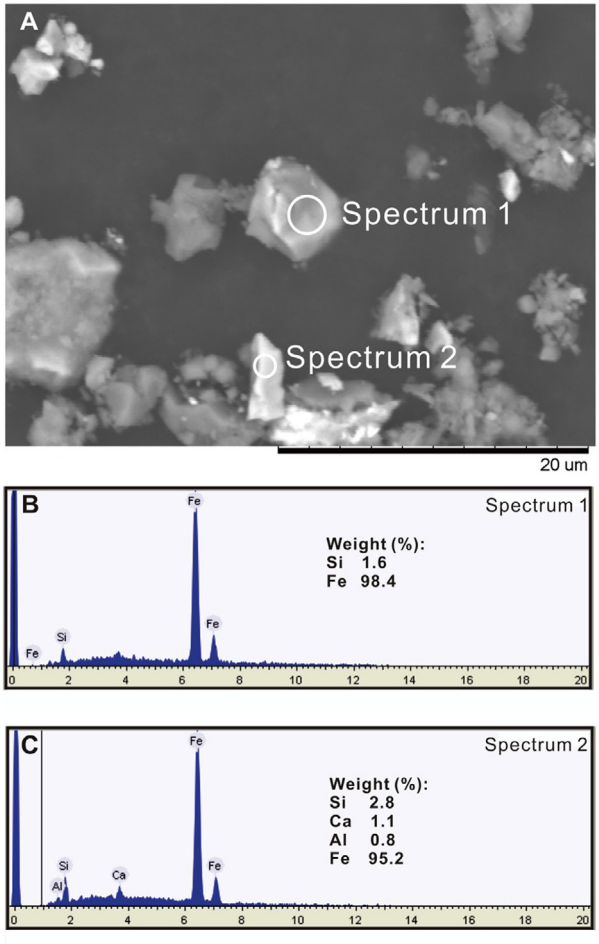

Fig. 13. (A) Representative SEM images. (B) and (C) EDS spectra of Fe oxides. White circles indicate the spots used for the EDS analyses. The weight % of each element is shown on the EDS spectra.

and Kodama, submitted for publication). The similar durations over the three continents supports a primary origin for the SE.

5.3. The onset age of the SE

Among the available age constraints for the SE, the U-Pb age of 551.1 ± 0.7 Ma obtained from an ash layer at the top of the black shale of the Doushantuo Formation in the Yangtze Gorges area has been regarded as the most robust estimate of the termination age of the SE globally (Condon et al., 2005; Le Guerroué et al., 2006; Fike et al., 2006; Zhu et al., 2007; Lu et al., 2013; Minguez et al., 2015). A recent Re-Os date for the base of the black shale in the Doushantuo Formation yields an age of 591.1 ± 5.3 Ma, suggesting that the black shale was deposited at least over a 40 Myr period (Zhu et al., 2013). This long depositional interval appears to require an unreasonably low accumulation rate for such a lithology. Besides, this Re-Os age of 591.1 ± 5.3 Ma is questioned by Kendall et al. (2015), who argue that post-depositional processes have affected the reliability of the data. Hence, we prefer the U-Pb age of 551.1 ± 0.7 Ma as the termination age of the SE.

Le Guerroué et al. (2006) suggest that the onset age of the SE is ca. 600 Ma based on the SHRIMP U-Pb detrital zircon age of 609 ± 7 Ma obtained from the Khufai Formation of the Huqf region, Oman. If it is true, the duration of the SE would be ~50 Myr. Although Le Guerroué et al. (2006) proposed a thermal subsidence model to explain the prolonged duration of the SE in Oman, this model is difficult to apply to other exposures of the SE given their different depositional environments and varied stratigraphic thicknesses (Lu et al., 2013). In addition, the detrital zircon data can only constrain the maximum onset age of the SE, hence the actual age could be considerably younger. Neither the proposed origin of the SE, including the oxidation of a large dissolved organic carbon (DOC) reservoir (Rothman et al., 2003), nor the massive release of methane hydrates (Bjerrum and Canfield, 2011) could accommodate a 50 Myr duration for the SE.

If we accept the 551.1 ± 0.7 Ma as the termination age of the SE and the ~9 Myr duration estimated from South China, North America and South Australia, the onset age of the SE would be ca. 560 Ma. In this scenario, the SE postdated the Gaskiers glaciation (ca. 580 Ma; Halverson et al., 2005) and the first appearance of the Ediacaran-type biota (ca. 575 Ma; Narbonne and Gehling, 2003), thus providing a robust chronostratigraphic framework for evaluating the relationship between the SE and the evolution of metazoans in Ediacaran time.

6. Conclusions

(1) Paleomagnetic study of the Doushantuo Formation at the Dongdahe section in eastern Yunnan Province, South China yields a paleomagnetic pole which lies close to the late Mesozoic paleomagnetic poles for South China, indicating a remagnetization. Detailed rock magnetic and SEM analyses show that detrital PSD or small MD titanomagnetite grains carrying the remanence have not been affected by the authigenesis and are able to record the orbitally-forced climate cycles in the Ediacaran. We speculate that samples acquired a stable thermoviscous remanent magnetization during the late Mesozoic Yanshanian orogeny in the Cretaceous normal polarity superchron in South China. But additional investigations are required for the magnetostratigraphy and paleogeography of the Doushantuo Formation.

(2) Multi-taper method spectral analysis of the MS and ARM series of the Doushantuo Formation reveals significant spectral peaks at predicted Ediacaran Milankovitch frequencies. The sediment accumulation rate of the Doushantuo Formation is estimated to be 1.0 cm/kyr, which gives the entire SE a duration of 9.1 ± 1.0 Myr. This duration is consistent with the results from North America and South Australia, reinforcing the suggestion of a primary origin for the SE. Combined with available geochronologic data, the onset age of the SE is suggested to be ca. 560 Ma, thus providing a robust chronostratigraphic framework for evaluating the relationship between the SE and the evolution of metazoans in the Ediacaran.

Acknowledgements

This study is supported by the National Science Foundation (EAR-1322002) and the National Natural Science Foundation of China (No. 41230208). We thank Gray Bebout, Frank Pazzaglia and Aihua Yang for helpful discussions; Bruce Idleman, Daniel Minguez, and Shipeng Wang for the laboratory and field assistances. We are grateful to John Geissman, Ross Mitchell and Sergei Pisarevsky for constructive and insightful reviews.

References

Abrajevitch, A., Van der Voo, R., 2010. Incompatible Ediacaran paleomagnetic directions suggest an equatorial geomagnetic dipole hypothesis. Earth Planet. Sci. Lett. 293 (1), 164–170.

Berger, A., Loutre, M.F., 1994. Astronomical forcing through geological time. Orbital forcing and cyclic sequences (IAS Special Publication), PL de Boer and DG Smith, eds, 19, 15–24.
Bjerrum, C.J., Canfield, D.E., 2011. Towards a quantitative understanding of the late Neoproterozoic carbon cycle. Proc. Natl. Acad. Sci. 108 (14), 5542–5547.
Bosscher, H., Schlager, W., 1993. Accumulation rates of carbonate platforms. J. Geol., 345–355
Bowring, S.A., Grotzinger, J.P., Condon, D.J., Ramezani, J., Newall, M.J., Allen, P.A., 2007. Geochronologic constraints on the chronostratigraphic framework of the Neoproterozoic Huqf Supergroup, Sultanate of Oman. Am. J. Sci. 307 (10), 1097–1145.
Boyden, J.A., Müller, R.D., Gurnis, M., Torsvik, T.H., Clark, J.A., Turner, M., et al., 2011. Next-generation plate-tectonic reconstructions using GPlates. Geoinformatics 9, 5–114.
Bristow, T.F., Kennedy, M.J., 2008. Carbon isotope excursions and the oxidant budget of the Ediacaran atmosphere and ocean. Geology 36 (11), 863–866.
Butler, R.F., Banerjee, S.K., 1975. Theoretical single-domain grain size range in magnetite and titanomagnetite. J. Geophys. Res. 80 (29), 4049–4058.
Canfield, D.E., Poulton, S.W., Narbonne, G.M., 2007. Late-Neoproterozoic deep-ocean oxygenation and the rise of animal life. Science 315 (5808), 92–95.
Cardozo, N., Allmendinger, R.W., 2013. Spherical projections with OSXStereonet. Comput. Geosci. 51, 193–205.
Condon, D., Zhu, M., Bowring, S., Wang, W., Yang, A., Jin, Y., 2005. U-Pb ages from the Neoproterozoic Doushantuo Formation, China. Science 308 (5718), 95–98.
Cui, H., Kaufman, A.J., Xiao, S., Zhu, M., Zhou, C., Liu, X.M., 2015. Redox architecture of an Ediacaran ocean margin: Integrated chemostratigraphic ($\delta^{13}C$-$\delta^{34}S$-$^{87}Sr/^{86}Sr$-Ce/Ce*) correlation of the Doushantuo Formation, South China. Chem. Geol. 405, 48–62.
Derry, L.A., 2010. A burial diagenesis origin for the Ediacaran Shuram-Wonoka carbon isotope anomaly. Earth Planet. Sci. Lett. 294 (1), 152–162.
Fike, D.A., Grotzinger, J.P., Pratt, L.M., Summons, R.E., 2006. Oxidation of the Ediacaran Ocean. Nature 444 (7120), 744–747.
Ghil, M., Allen, M.R., Dettinger, M.D., Ide, K., Kondrashov, D., Mann, M.E., Yiou, P., 2002. Advanced spectral methods for climatic time series. Rev. Geophys. 40 (1). 3-1.
Grotzinger, J.P., Fike, D.A., Fischer, W.W., 2011. Enigmatic origin of the largest-known carbon isotope excursion in Earth's history. Nat. Geosci. 4 (5), 285–292.
Halverson, G.P., Hoffman, P.F., Schrag, D.P., Maloof, A.C., Rice, A.H.N., 2005. Toward a Neoproterozoic composite carbon-isotope record. Geol. Soc. Am. Bull. 117 (9–10), 1181–1207.
Hinnov, L.A., 2000. New perspectives on orbitally forced stratigraphy. Annu. Rev. Earth Planet. Sci. 28 (1), 419–475.
Hounslow, M.W., Maher, B.A., 1999. Laboratory Procedures for Quantitative Extraction and Analysis of Magnetic Minerals from Sediments. Environmental Magnetism: A Practical Guide. Quaternary Research Association, Cambridge, UK, pp. 139–184.
Huang, B.C., Zhou, Y.X., Zhu, R.X., 2008. Discussions on Phanerozoic evolution and formation of continental China, based on paleomagnetic studies. Earth Sci. Front. 15 (3), 348–359.
Jackson, M., Gruber, W., Marvin, J., Banerjee, S.K., 1988. Partial anhysteretic remanence and its anisotropy: Applications and grain size-dependence. Geophys. Res. Lett. 15 (5), 440–443.
Jiang, G., Kaufman, A.J., Christie-Blick, N., Zhang, S., Wu, H., 2007. Carbon isotope variability across the Ediacaran Yangtze platform in South China: implications for a large surface-to-deep ocean $\delta^{13}C$ gradient. Earth Planet. Sci. Lett. 261 (1), 303–320.
Jiang, G., Shi, X., Zhang, S., Wang, Y., Xiao, S., 2011. Stratigraphy and paleogeography of the Ediacaran Doushantuo Formation (ca. 635–551 Ma) in South China. Gondwana Res. 19 (4), 831–849.
Jing, X.Q., Yang, Z., Tong, Y., Han, Z., 2015. A revised paleomagnetic pole from the mid-Neoproterozoic Liantuo Formation in the Yangtze block and its paleogeographic implications. Precambr. Res. 268, 194–211.
Kendall, B., Komiya, T., Lyons, T.W., Bates, S.M., Gordon, G.W., Romaniello, S.J., Sawaki, Y., 2015. Uranium and molybdenum isotope evidence for an episode of widespread ocean oxygenation during the late Ediacaran Period. Geochim. Cosmochim. Acta 156, 173–193.
Kirschvink, J.L., 1980. The least-squares line and plane and the analysis of palaeomagnetic data. Geophys. J. Int. 62 (3), 699–718.
Knauth, L.P., Kennedy, M.J., 2009. The late Precambrian greening of the Earth. Nature 460 (7256), 728–732.
Knoll, A., Walter, M., Narbonne, G., Christie-Blick, Nicholas, 2006. The Ediacaran Period: a new addition to the geologic time scale. Lethaia 39 (1), 13–30.
Kodama, K.P., Hinnov, L.A., 2014. Rock Magnetic Cyclostratigraphy. John Wiley & Sons.
Kodama, K.P., Anastasio, D.J., Newton, M.L., Pares, J.M., Hinnov, L.A., 2010. High-resolution rock magnetic cyclostratigraphy in an Eocene flysch, Spanish Pyrenees. Geochem. Geophys. Geosyst. 11 (6).
Kruiver, P.P., Dekkers, M.J., Heslop, D., 2001. Quantification of magnetic coercivity components by the analysis of acquisition curves of isothermal remanent magnetization. Earth Planet. Sci. Lett. 189 (3), 269–276.
Laskar, J., Robutel, P., Joutel, F., Gastineau, M., Correia, A.C.M., Levrard, B., 2004. A long-term numerical solution for the insolation quantities of the Earth. Astron. Astrophys 428 (1), 261–285. Chicago.
Laskar, J., Fienga, A., Gastineau, M., Manche, H., 2011. La2010: a new orbital solution for the long-term motion of the Earth. Astron. Astrophys. 532, A89.
Le Guerroué, E., Allen, P.A., Cozzi, A., Etienne, J.L., Fanning, M., 2006. 50 Myr recovery from the largest negative $\delta^{13}C$ excursion in the Ediacaran ocean. Terra Nova 18 (2), 147–153.
Li, Z.X., Bogdanova, S.V., Collins, A.S., Davidson, A., De Waele, B., Ernst, R.E., Karlstrom, K.E., 2008. Assembly, configuration, and break-up history of Rodinia: a synthesis. Precambr. Res. 160 (1), 179–210.
Liang, Q.Z. et al., 1984. Report on the Regional Geological Investigation of the Kunming District. Yunnan Geological Bureau, Kunming, China.
Lowrie, W., 1990. Identification of ferromagnetic minerals in a rock by coercivity and unblocking temperature properties. Geophys. Res. Lett. 17 (2), 159–162.
Lu, M., Zhu, M., Zhang, J., Shields-Zhou, G., Li, G., Zhao, F., Zhao, M., 2013. The DOUNCE event at the top of the Ediacaran Doushantuo Formation, South China: broad stratigraphic occurrence and non-diagenetic origin. Precambr. Res. 225, 86–109.
Lurcock, P.C., Wilson, G.S., 2012. PuffinPlot: a versatile, user-friendly program for paleomagnetic analysis. Geochem. Geophys. Geosyst. 13 (6).
Macouin, M., Besse, J., Ader, M., Gilder, S., Yang, Z.Y., Sun, Z., Agrinier, P., 2004. Combined paleomagnetic and isotopic data from the Doushantuo carbonates, South China: implications for the "snowball Earth" hypothesis. Earth Planet. Sci. Lett. 224 (3), 387–398.
Mann, M.E., Lees, J.M., 1996. Robust estimation of background noise and signal detection in climatic time series. Clim. Change 33 (3), 409–445.
McCabe, C., Van der Voo, R., Peacor, D.R., Scotese, C.R., Freeman, R., 1983. Diagenetic magnetite carries ancient yet secondary remanence in some Paleozoic sedimentary carbonates. Geology 11 (4), 221–223.
McFadden, K.A., Huang, J., Chu, X., Jiang, G., Kaufman, A.J., Zhou, C., Xiao, S., 2008. Pulsed oxidation and biological evolution in the Ediacaran Doushantuo Formation. Proc. Natl. Acad. Sci. 105 (9), 3197–3202.
Melezhik, V.A., Pokrovsky, B.G., Fallick, A.E., Kuznetsov, A.B., Bujakaite, M.I., 2009. Constraints on $^{87}Sr/^{86}Sr$ of Late Ediacaran seawater: insight from Siberian high-Sr limestones. J. Geol. Soc. 166 (1), 183–191.
Minguez, D., Kodama, K.P., 2016. Rock magnetic cyclostratigraphy and magnetostratigraphy of the Wonoka Formation, Australia: Duration and possible global synchroneity of the Shuram carbon isotope excursion. Manuscript submitted for publication.
Minguez, D., Kodama, K.P., Hillhouse, J.W., 2015. Paleomagnetic and cyclostratigraphic constraints on the synchroneity and duration of the Shuram carbon isotope excursion, Johnnie Formation, Death Valley Region, CA. Precambr. Res. 266, 395–408.
Narbonne, G.M., Gehling, J.G., 2003. Life after snowball: the oldest complex Ediacaran fossils. Geology 31 (1), 27–30.
Paillard, D., 1996. Macintosh Program Performs Time-Series Analysis. Eos Trans, AUG.
Rothman, D.H., Hayes, J.M., Summons, R.E., 2003. Dynamics of the neoproterozoic carbon cycle. Proc. Natl. Acad. Sci. 100 (14), 8124–8129.
Suk, D., Peacor, D.R., Van der Voo, R., 1990. Replacement of pyrite framboids by magnetite in limestone and implications for palaeomagnetism. Nature 345 (6276), 611–613.
Thomson, D.J., 1982. Spectrum estimation and harmonic analysis. Proc. IEEE 70 (9), 1055–1096.
Waltham, D., 2015. Milankovitch period uncertainties and their impact on cyclostratigraphy. J. Sediment. Res. 85 (8), 990–998.
Wang, J., Li, Z.X., 2003. History of neoproterozoic rift basins in South China: implications for Rodinia break-up. Precambr. Res. 122 (1), 141–158.
Weedon, G.P., 2003. Time-Series Analysis and Cyclostratigraphy: Examining Stratigraphic Records of Environmental Cycles. Cambridge University Press.
Wu, H., Zhang, S., Feng, Q., Jiang, G., Li, H., Yang, T., 2012. Milankovitch and sub-Milankovitch cycles of the early Triassic Daye Formation, South China and their geochronological and paleoclimatic implications. Gondwana Res. 22 (2), 748–759.
Zhang, S., Li, H., Jiang, G., Evans, D.A., Dong, J., Wu, H., Xiao, Q., 2015. New paleomagnetic results from the Ediacaran Doushantuo Formation in South China and their paleogeographic implications. Precambr. Res. 259, 130–142.
Zhang, Y., Jia, D., Yin, H., Liu, M., Xie, W., Wei, G., Li, Y., 2016. Remagnetization of lower Silurian black shale and insights into shale gas in the Sichuan Basin, South China. J. Geophys. Res. Solid Earth.
Zhu, M., Zhang, J., Yang, A., 2007. Integrated Ediacaran (Sinian) chronostratigraphy of South China. Palaeogeogr. Palaeoclimatol. Palaeoecol. 254 (1), 7–61.
Zhu, B., Becker, H., Jiang, S.Y., Pi, D.H., Fischer-Gödde, M., Yang, J.H., 2013. Re-Os geochronology of black shales from the Neoproterozoic Doushantuo Formation, Yangtze platform, South China. Precambr. Res. 225, 67–76.
Zijderveld, J.D.A., 1967. AC demagnetization of rocks: analysis of results. Methods Paleomagnetism 3, 254.